Scanning Microscopy

Volume 7 | Number 1 Article 27

12-30-1992

Calcospherites in Rabbit Incisor Predentin

H. Mishima
Nihon University of Dentistry at Matsudo

Y. Kunuki
Nihon University of Dentistry at Matsudo

T. Sakae
Nihon University of Dentistry at Matsudo

Y. Kozawa
Nihon University of Dentistry at Matsudo

N. Watabe
University of South Carolina, Columbia

Scanning Microscopy, Vol. 7, No. 1, 1993 (Pages 255-265)
Scanning Microscopy International, Chicago (AMF O'Hare), IL 60666 USA

0891-7035/93$5.00+.00

CALCOSPHERITES IN RABBIT INCISOR PREDENTIN

H. Mishima[1*], Y. Kunuki[1], T. Sakae[1], Y. Kozawa[1] and N. Watabe[2]

[1]Department of Anatomy, Nihon University School of Dentistry at Matsudo, Chiba 271, Japan
[2]Electron Microscopy Center, University of South Carolina, Columbia, S.C. 29208, U.S.A.

(Received for publication May 4, 1992, and in revised form December 30, 1992)

Abstract

Calcospherites from the lower incisor dentin of rabbits were investigated by scanning and transmission electron microscopy (TEM), energy dispersive spectroscopy (EDS) and electron diffraction analyses. In the labial predentin, globular calcospherites of 8-31 μm were present at the root apex, decreasing in size toward the incisal region. The calcospherites at the intermediate region were of mulberry- as well as of spindle-shape of 1.5-4 μm diameter. The incisal pulp horn contained micro-calcospherites of 0.3-0.6 μm in diameter. In the lingual predentin, small granular calcospherites of 1.8-3 μm were present at the root apex, increasing in size toward the intermediate region. Ultrathin sections of globular calcospherites showed bundles of collagen fibrils at the root apex of the labial predentin. The diameters of individual bundles ranged from 1.2-3.4 μm. The width of the fibrils in the bundles was approximately 120-170 nm. Bundles of collagen fibrils were not found in the lingual predentin. Crystals of calcospherites were identified as apatite by electron diffraction. Those at the intermediate region showed preferred orientation of the c-axis. TEM-EDS analyses indicated that Ca and P were the major elements, with small amounts of Mg. The Mg/Ca molar ratios decreased from the root apex to the incisal pulp horn. Ca peak intensities increased from the root apex to the incisal region.

Key Words: Dentin, rabbit, calcospherite, scanning electron microscopy, transmission electron microscopy, energy dispersive spectroscopy, electron diffraction.

*Address for correspondence:
H. Mishima
Department of Anatomy,
Nihon University School of Dentistry at Matsudo,
2-870-1 Sakaecho-Nishi, Matsudo,
Chiba 271, Japan

Phone No.:0473-68-6111 Ext. 386
FAX No.:0473-64-6295

Introduction

In incisor dentins, differences are found in the crystal orientation [24], dentin structure [23, 25, 29], calcification pattern [26], organic matrix composition [3, 36, 39], or inorganic composition [9, 34, 40] between the labial (enamel covered dentin) and the lingual dentin (cementum covered dentin). The two dentins also show variations in the odontoblasts structure [16, 41]. Beertsen and Niehof [4] report that the morphology of secretory granules of the odontoblast layer is different between the labial dentin and lingual dentin.

Although the initial mineralization in dentinogenesis has been studied extensively [1, 5-8, 10, 13-15, 22, 38, 42], there are no reports on the formation of calcospherites in secondary circumpulpal dentinogenesis. In the rabbit incisor predentin, the shape and size of calcospherites vary extensively at the intermediate region between the root apex and the incisal pulp horn [27]. This paper reports the results of scanning and transmission electron microscopic investigations of calcospherites in the predentin of rabbit incisors. Elemental compositions and crystallographic characteristics obtained by energy dispersive X-ray microanalysis (EDS) and electron diffraction analysis are also discussed.

Materials and Methods

Bilateral lower incisors from ten male Japanese white rabbits weighing 2.5 to 3.5 kg each were used in the present study. Six rabbits were decapitated after Nembutal anesthesia. These lower incisors were extracted and immediately fixed in 10% neutral formaldehyde solution for 24 hours. After the fixation, the incisors were cut transversely into three portions with a torx dental turbine (Morita Co. Ltd., Tokyo) equipped with a diamond disc. They were divided further, with the same turbine, into separate labial and lingual dentin, and treated with NaOCl to expose the mineralization front. The specimens were kept in fresh 10% NaOCl solution for 30 minutes at room temperature with gentle agitation, and rinsed thoroughly with distilled water. The specimens were dehydrated in a series of ethanols, substituted with isoamyl acetate, and subjected to critical-

point drying with carbon dioxide. The pulpal surfaces were gold-coated in an ion coater and observed with a JEOL JSM-T200 and a HITACHI S-2500Δ operated at an accelerating voltage of 25 kV.

For transmission electron microscopy (TEM), four rabbits were anesthetized with Nembutal and perfused through the aorta with Tyrode's solution, followed by 2% glutaraldehyde in 0.05 M cacodylate, pH 7.4. After the perfusion, the incisors were immersed in the same fixative for 24 hours and washed with the same buffer. The root apex of the incisor was sliced transversely into smaller pieces with a razor blade. The other incisal part of the incisor was cut transversely into smaller pieces with the dental turbine. These specimens were postfixed with 1% osmium tetroxide in 0.05 M cacodylate buffer, and rinsed again in the same buffer. They were dehydrated in a series of ethanols, transferred into propylene oxide, and embedded in epoxy resin (Quetol 812) without decalcification. Thin sections ($\sim$ 0.1 μm in thickness) were cut with a diamond knife using a Sorval MT2-B ultramicrotome, unstained or stained with 5% uranyl acetate and 1% lead citrate, or 1% lead citrate only, and examined with a HITACHI H-8000 transmission electron microscope operated at 100 kV. The plane of section used for TEM was transverse to the incisor axis. Energy dispersive X-ray microanalysis was carried out on about 1 μm^2 areas of unstained calcospherite in the nano-probe mode with a Kevex system attached to the TEM. Analytical conditions were: accelerating voltage, 100 kV; beam-sample incidence angle, 90°; X-ray emergence angle, 59.8°; X-ray-window incidence angle, -8.2°; counting time, 200 seconds; magnification, x 10,000. X-ray spectra were analyzed using a Kevex Delta computer program (thin film analysis) and data expressed as atomic percentages for each element detected. The regions of EDS analyses were 7 roughly equally spaced consecutive areas from the root apex to the incisal pulp horn (Fig. 1). An average of 5 different spots were analyzed in one area. Electron diffraction analysis was performed at 100 kV on unstained 3.3 μm diameter areas.

Results

Scanning electron microscopy

The morphologies of calcospherites observed after the NaOCl treatment front from the root apex to the incisal pulp horn of the incisor are as follows.

Labial dentin. Calcospherites are globular and 8-31 μm in diameter at the root apex, and contain from 2 to 9 dentinal tubules (dt) (Figures 2 and 3). Sometimes, surfaces of the calcospherites are covered with collagen fibers left undigested by the NaOCl treatment. The size of the calcospherite decreases toward the incisal direction. The calcospherites change from globular to mulberry-shape at the intermediate region between the root apex and the incisal pulp horn (Figure 4). The size of mulberry-shape calcospherites ranges from 5-10 μm. Figure 5 shows micro-calcospherites of 0.3-0.6 μm at the incisal pulp horn.

Lingual dentin. At the root apex, calcospherites are small and granular (1.8-3 μm) (Figure 6), and have flaky to needle-like crystals on their surfaces (Figure 7). The morphology changes from granular to ridge-like toward the incisal direction. At the intermediate region, it transforms from ridge-like to spindle-shape (Figure 8), and the size is larger (2-10 μm) than that at the root apex. The incisal pulp horn contains micro-calcospherites of 0.3-0.6 μm (Figure 9). At the incisal pulp horn, the shape and size of calcospherites is similar in the labial predentin and lingual predentin.

Transmission electron microscopy

Labial dentin. Ultrathin sections stained with lead citrate showed globular calcospherites and bundles of collagen fibrils at the root apex of the labial predentin (Figure 10). Obliquely sectioned bundles of collagen fibrils (circle) were scattered in the matrix region. The diameter of individual bundles ranged from 1.2-3.4 μm. Needle-like crystals were observed within and adjacent to the collagen bundles (Figures 10 and 11). The calcospherites around the mineralization front were 1.9-5.1 μm in diameter and consisted of randomly oriented crystals (Figure 12). The crystals were 95-131 nm long, and approximately 11 nm wide. Collagen fibrils showing a periodicity of about 64 nm were present in the calcospherite. Uranyl acetate staining demineralized crystals in calcospherites and revealed thick collagen fibrils approximately 80-143 nm wide within and around the collagen bundles (arrows, Figure 13). The predentin matrix showed a dense population of randomly oriented collagen fibrils of small diameter (50-90 nm). Figure 14 showed fused calcospherites at the intermediate region. The calcospherites were from 1-11 μm in diameter and contained 2 to 4 odontoblast processes (arrows). The size of the calcospherites decreased toward the incisal region. Micro-calcospherites of 140-670 nm at the incisal pulp horn are shown in Figure 15.

Lingual dentin. Sections stained with lead citrate show micro-calcospherites of 170-990 nm in diameter at the root apex (Figure 16). In the predentin, bundles of collagen fibrils were not evident, and the matrix showed a small population of regularly oriented collagen fibrils 40-80 nm wide (Figure 17). Needle-like crystals, 64-128 nm long and 8-12 nm wide, were observed within and adjacent to the collagen fibrils. The calcospherites increased in size ranging from 140 nm to 1.7 μm, toward the intermediate region (Figure 18) and showed micro-calcospherites, 110-680 nm, at the incisal pulp horn (Figure 19).

TEM-EDS analysis and electron diffraction analysis of calcospherites

EDS analysis of calcospherites showed that Ca and P are the major elements, with small amounts of Mg, Cl and Os. Cl from the epoxy resin, Os from the fixative, and Cu from the specimen grid were also detected. The Mg/Ca molar ratio of labial calcospherites was higher than that of lingual calcospherites at the root

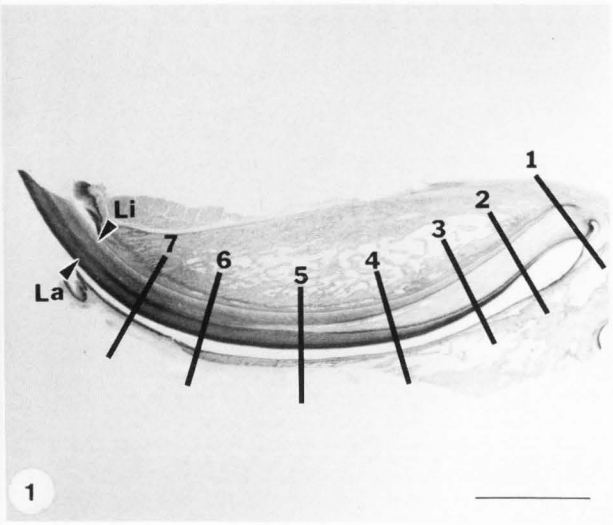

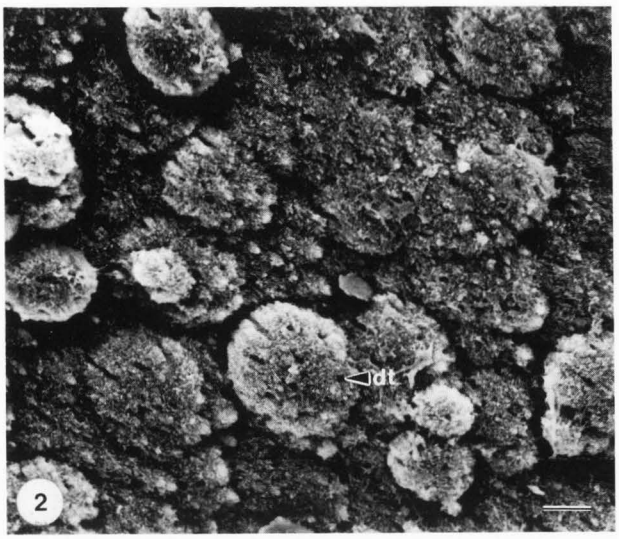

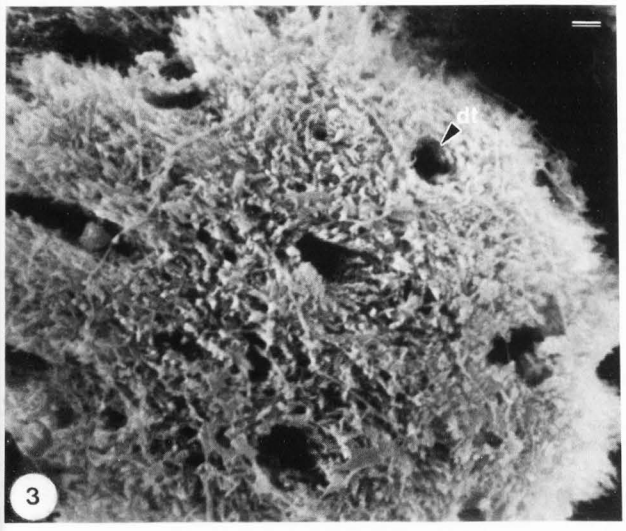

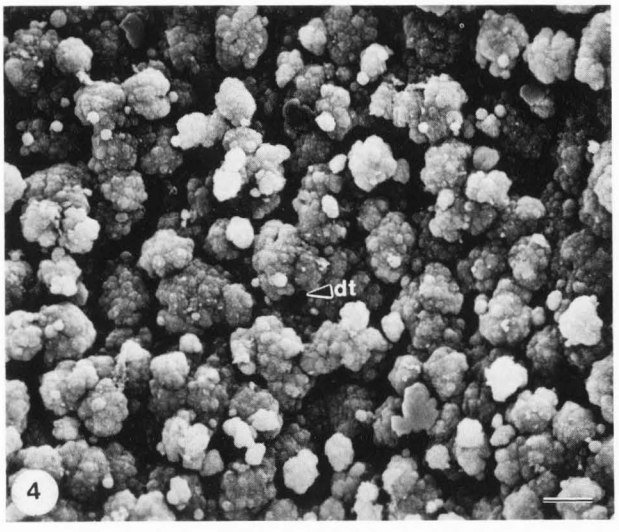

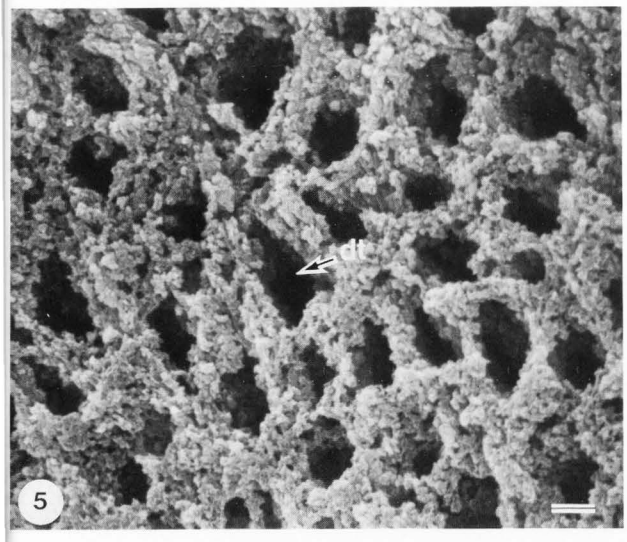

Figure 1. Longitudinal section of a rabbit lower incisor. Numbers (1-7) indicate areas of EDS analyses referred to in the text. This specimen was used in Numata and Mishima [29]. La: labial dentin, Li: lingual dentin. Bar = 5 mm.

Figure 2. Scanning electron micrograph of globular calcospherites of labial predentin. Root apex. dt: dentinal tubules. Bar = 10 μm.

Figure 3. The calcospherites contain 9 dentinal tubules (dt). Bar = 1μm.

Figure 4. Scanning electron micrograph of mulberry-shape calcospherites of labial predentin. Intermediate region. Bar = 10 μm.

Figure 5. Scanning electron micrograph of micro-calcospherites of labial predentin. Incisal pulp horn. Bar = 2 μm.

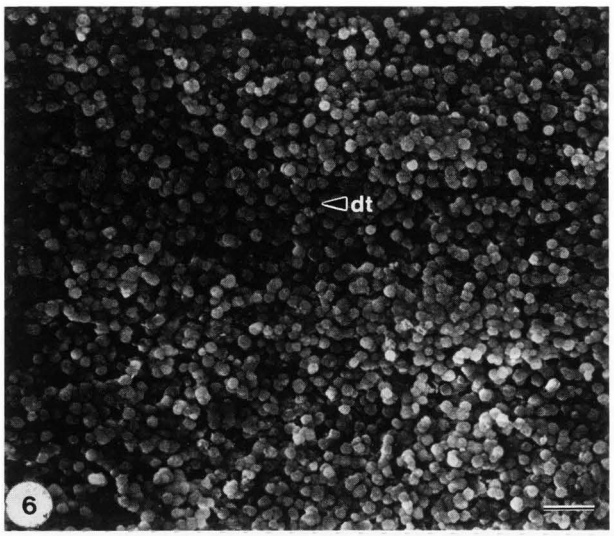

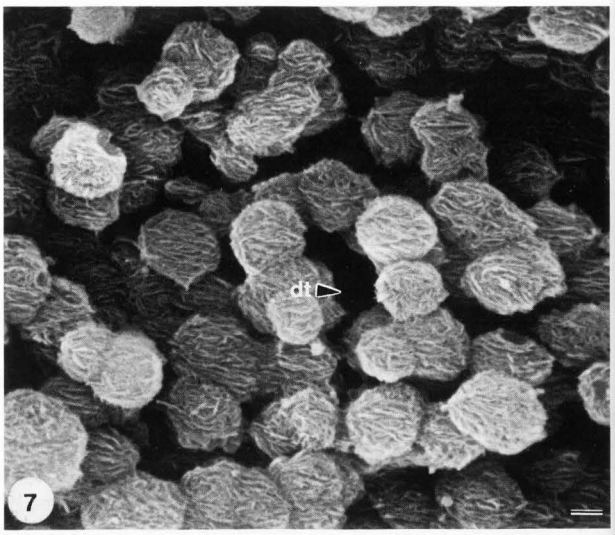

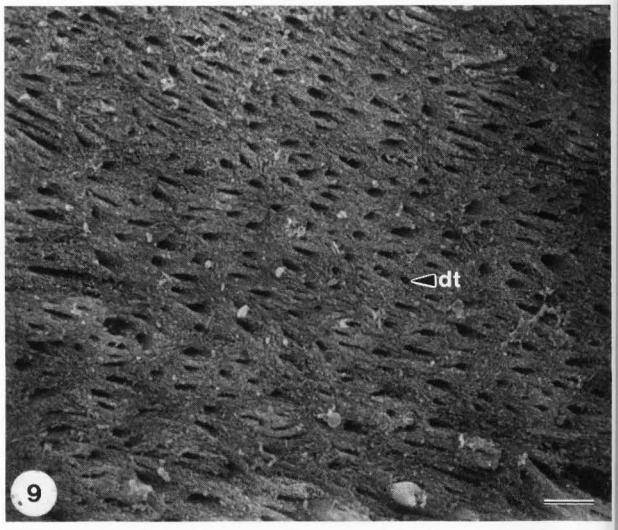

apex (Figure 20). The Ca/P molar ratio of labial calcospherites was lower than that of lingual calcospherites at the root apex (Figure 21). The Ca/P molar ratios of labial calcospherites were 2.02 $\pm$ 0.194 (n = 40) and those of lingual calcospherites were 2.04 $\pm$ 0.174 (n = 40). In the intermediate region, the Mg/Ca molar ratio of lingual calcospherites was higher than that of labial calcospherites. In both labial and lingual calcospherites, Mg/Ca molar ratios were reduced from the root apex to the incisal pulp horn. In contrast, Ca peak intensities increased from the root apex to the incisal pulp horn (Figure 22).

Selected area electron diffractions of the areas where the EDS was performed showed that crystals correspond to hydroxyapatite (Figures 23-26, Table 1). The diffraction patterns of the root apex indicated random crystal orientation (Figures 23 and 24), whereas those of the intermediate regions showed preferred orientation of the c-axis (arrows, Figures 25 and 26). The direction of the orientation was from the intermediate region to the incisal pulp horn.

Figure 6. Scanning electron micrograph of small granular calcospherites of lingual predentin. Root apex. Bar = 10 μm.

Figure 7. Flaky to needle-like crystals on the surface of calcospherites. Bar = 1 μm.

Figure 8. Scanning electron micrograph of spindle-shape calcospherites of lingual predentin. Intermediate region. Bar = 10 μm.

Figure 9. Scanning electron micrograph of micro-calcospherites of lingual predentin. Incisal pulp horn. Bar = 10 μm.

Discussion

For the first time, the present study showed that the morphology of calcospherites in the incisor predentin varies from the root apex to the incisal pulp horn. In the labial predentin, globular calcospherites were present

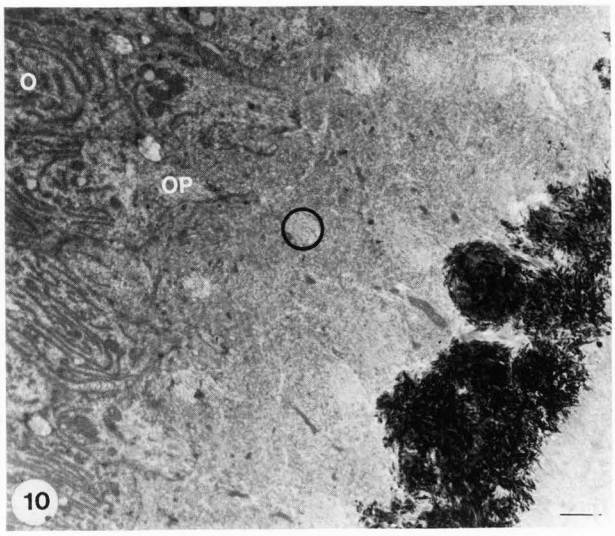

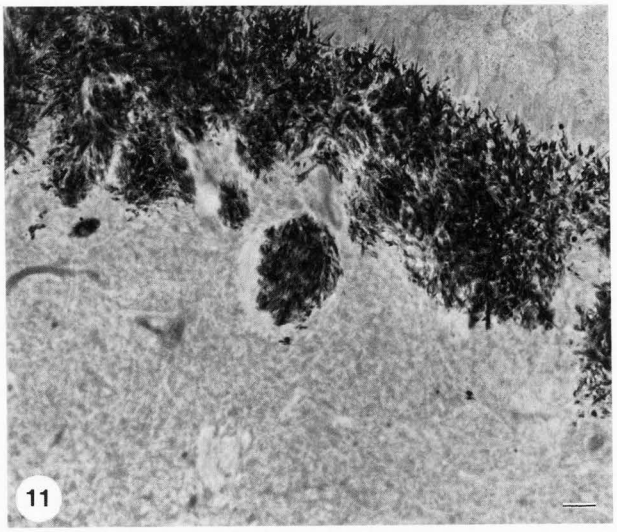

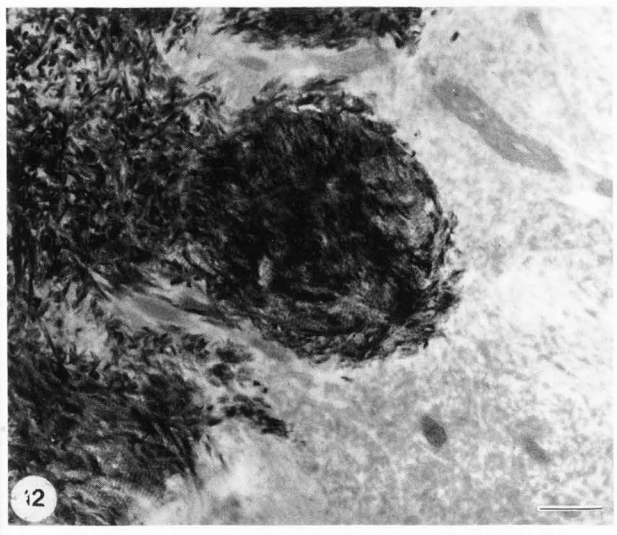

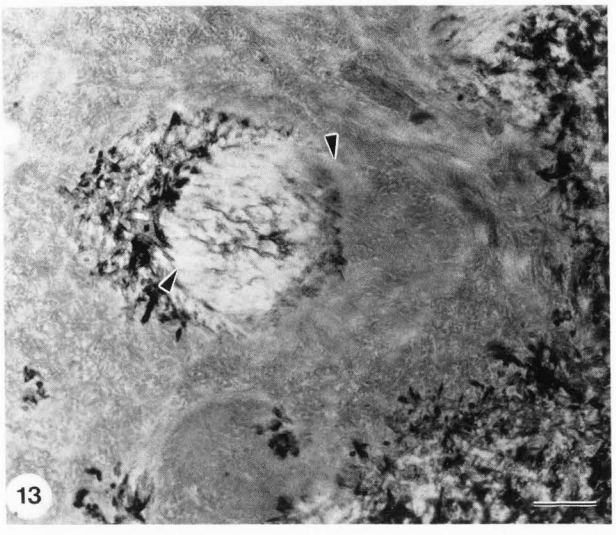

Figure 10. Transmission electron micrograph of globular calcospherites and bundles of collagen fibrils of labial predentin. Root apex. Stained with lead citrate. O: odontoblast, OP: odontoblast process, circle: bundles of collagen fibrils. Bar = 2 μm.

Figure 11. Needle-like crystals within the collagen bundles. Stained with lead citrate. Bar = 1 μm.

Figure 12. Transmission electron micrograph of calcospherites of labial predentin. Root apex. Stained with lead citrate. Bar = 1 μm.

Figure 13. Thick collagen fibrils within and around the collagen bundles. Stained with uranyl acetate and lead citrate. Arrows: thick collagen fibrils. Bar = 1 μm.

---

at the root apex, decreasing in size toward the incisal pulp horn. In the lingual predentin, small granular calcospherites were present at the root apex, increasing in size toward the intermediate region. The incisal pulp horn of both labial and lingual dentin contained microcalcospherites.

Mummery [28] reported that calcospherites assumed two forms: those with radial striae, and those with concentric lamellae or rings. Schmidt and Keil [35] concluded that within calcospherites the crystals were radially oriented. Shellis [37] showed in human dentin calcospherites that about half the crystals were radially oriented and other half were parallel to the collagen fibers. However, radially oriented crystals were not evident in our study. Observations of serial sections would reveal detailed information on crystal orientations in the calcospherites.

The diffraction patterns of calcospherites in all regions were similar to that of hydroxyapatite listed in the ASTM file. These patterns indicated no evidence of amorphous calcium phosphate, brushite (DCPD) or octacalcium phosphate (OCP). LeGeros *et al.* [19] reported the Ca/P molar ratios of synthetic DCPD was 1.0, OCP was 1.33, whitlockite (β-TCMP) ranged from 1.20 to 1.47, and CO_3-substituted apatite (CHA) ranged from 1.65 to 2.33. The Ca/P molar ratios of labial calcospherites, by our EDS analyses, were 2.02 $\pm$ 0.194 and

14

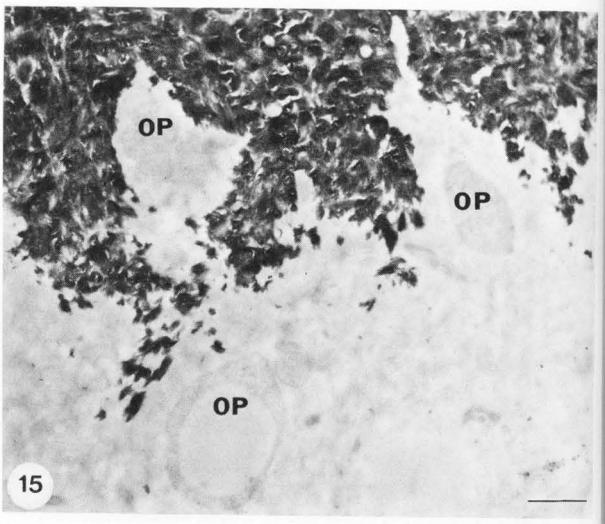

15

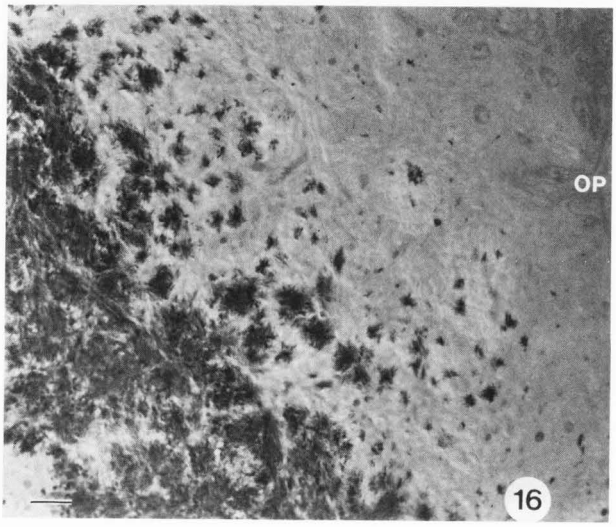

16

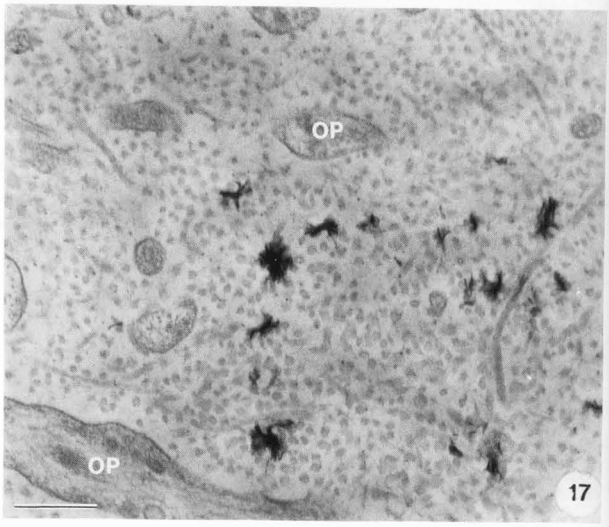

17

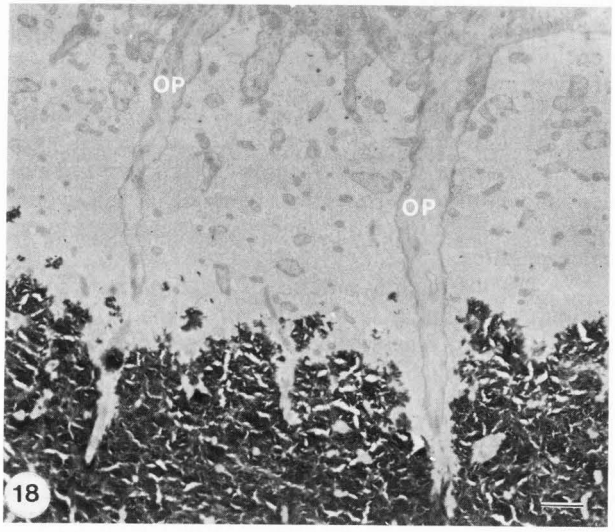

18

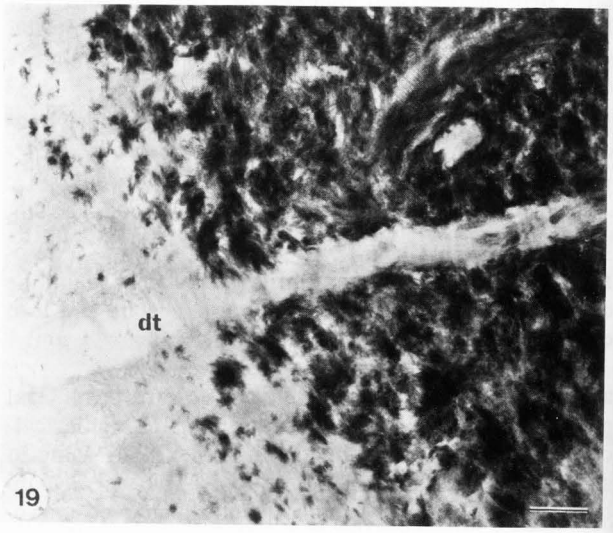

19

Figure 14. Transmission electron micrograph of fused calcospherites of labial predentin. Intermediate region. Arrow: odontoblast process. Stained with lead citrate. Bar = 1 μm.

Figure 15. Transmission electron micrograph of microcalcospherites of labial predentin. Incisal pulp horn. Op: odontoblast process. Stained with lead citrate. Bar = 1 μm.

Figure 16. Transmission electron micrograph of small granular calcospherites of lingual predentin. Root apex. Op: odontoblast process. Stained with lead citrate. Bar = 1 μm.

Figure 17. Needle-like crystals within and adjacent to the collagen fibrils. Op: odontoblast process. Stained with uranyl acetate and lead citrate. Bar = 500 nm.

Figure 18. Transmission electron micrograph of calcospherites of lingual predentin. Intermediate region. OP: odontoblast processes. Stained with lead citrate. Bar = 1 μm.

Figure 19. Transmission electron micrograph of microcalcospherites of lingual predentin. Incisal pulp horn. dt: dentinal tubules. Stained with lead citrate. Bar = 1 μm.

Figure 20. Mg/Ca molar ratios by EDS analysis in calcospherites. Numbers (1-7) corresponds to the regions of Fig. 1.

Figure 21. Ca/P molar ratios by EDS analysis in calcospherites. Numbers (1-7) Corresponds to the regions of Fig. 1.

Figure 22. Ca peak intensities by EDS analysis in calcospherites. Numbers (1-7) corresponds to the regions of Fig. 1.

---

those of lingual calcospherites 2.04 $\pm$ 0.174. These values correspond to those of CHA by LeGeros *et al.* [19]. Accordingly, our crystals can be assumed to be CO_3-substituted apatite instead of hydroxyapatite. The published diffraction patterns of those two minerals are similar [19]. In epiphyseal growth plates, initial enamel deposits, dentin mineralization front, and calcified dentins, crystals were apatite [2, 11, 12, 17]. CHA could assume morphologies from needle-like to rods to equiaxed crystal depending on the amount of CO_3 incorporated [19]. CHA or biological apatite are always associated with Mg [18]. Mg ions have been suggested as substitute for Ca ions in the apatite crystal to a limited extent [18-21, 30-32]. Our EDS analysis showed that Mg was present besides the main components (Ca and P) in the calcospherites. The correlation between the high value of the Mg/Ca molar ratio and the low value of the Ca/P molar ratio at the labial root apex suggests that Mg substitutes for Ca. The Mg/Ca ratio of calcospherites decreased from the root apex (initial dentin formation) to the incisal pulp horn (mature dentin formation), meanwhile Ca peak intensities increased from the root apex to the incisal pulp horn. This indicates that the Mg contents were higher at the initial stage of calcification, and

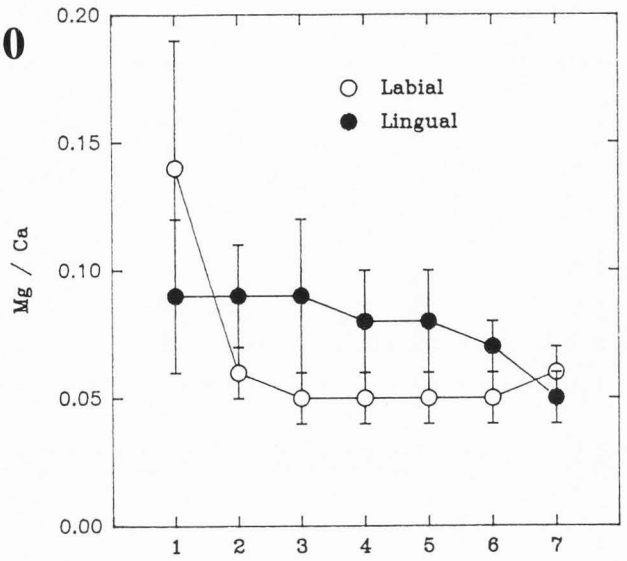

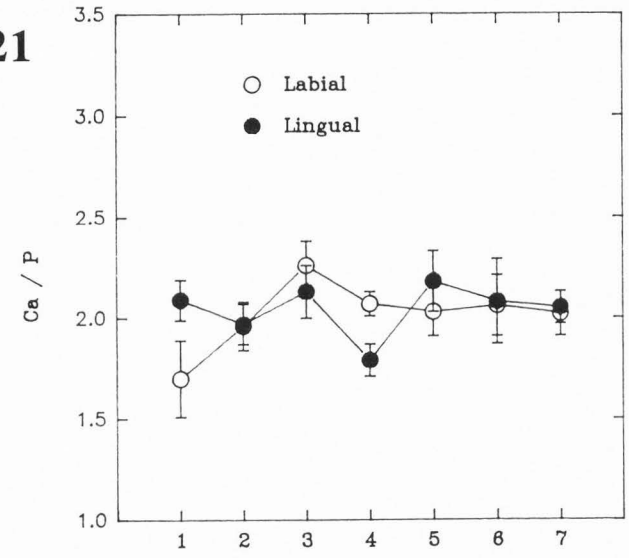

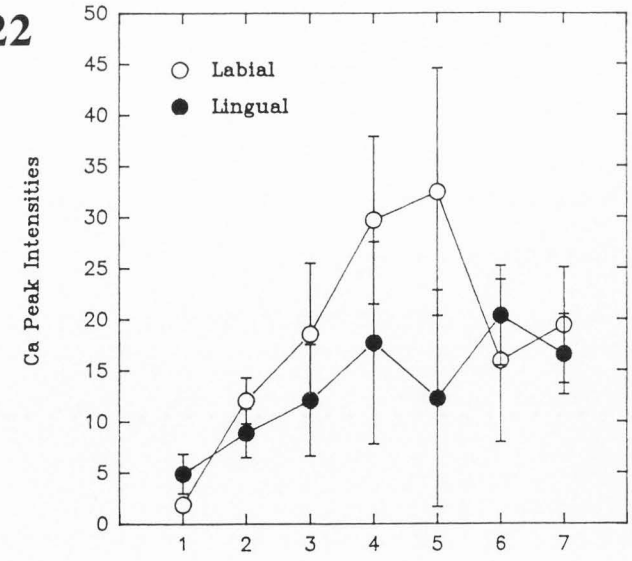

Table 1. D-spacings of calcospherites and hydroxyapatite

hkl	hydroxyapatite (ASTM 9-432) d(Å)	I	labial root apex (Fig. 23) d(Å)	lingual root apex (Fig. 24) d(Å)	labial intermediate (Fig. 25) d(Å)	lingual intermediate (Fig.26) d(Å)
002	3.44	40	3.39	3.45	3.42	3.40
102	3.17	11		3.14	3.16	
210	3.08	17	3.07			
211	2.814	100		2.81	2.81	
112	2.778	60	2.76			2.77
300	2.720	60				
202	2.631	25			2.66	
301	2.528	5				
212	2.296	7				
310	2.262	20	2.26	2.28	2.30	2.26
221	2.228	1				
311	2.148	9				
302	2.134	3				
113	2.065	7				
400	2.040	1				
203	2.000	5				
222	1.943	30	1.95	1.94	1.97	1.94
312	1.890	15				
320	1.871	5				
213	1.841	40	1.84	1.84	1.84	1.84
321	1.806	20				
410	1.780	11				
402, 303	1.754	15				
004, 411	1.722	20	1.71	1.71	1.71	1.72

agrees with LeGeros [21] and Okazaki [30, 32] that Mg may play an important role in the initial formation of dentin apatite; they suggested that Mg significantly affects the physicochemical stability of apatite crystals.

Large globular calcospherites were found in association with the bundles of collagen fibrils, having the same orientation, in the labial predentin. The odontoblasts probably produced the collagen bundles as well as the collagen fibrils of dentin matrix. Onozato and Watabe [33] reported, in scales of the goldfish, that the orientation of the collagen fibers of the sheets and lamellae seemed to be controlled by the orientation of the ridges and invaginations of the surface of the fibroblasts. The topography and orientation of the surface structure of the odontoblasts may determine the orientation of the collagen bundles and dentin matrix fibers.

Acknowledgements

A portion of this work was supported by the funds of Electron Microscopy Center, University of South Carolina. We thank the staff of the Department of Anatomy, Nihon University School of Dentistry at Matsudo, for their instruction and assistance, and to Dana Dunkelberger at the Electron Microscopy Center, University of South Carolina, for his technical assistance.

References

1. Avery JK (1986). Dentin. In: Orban's Oral Histology and Embryology. Bhasker SN (ed.), 10th edn., The CV Mosby Company, St. Louis, pp.101-134.

2. Barckhaus RH, Höhling HJ, Fromm I, Hirsh P, Reimer L (1991). Electron spectroscopic diffraction and imaging of the early and mature stages of calcium phosphate formation in the epiphyseal growth plate. J Microsc **162**: 155-169.

3. Beertsen W, Neihof A, Everts V (1985). Effects of 1-Hydroxyethlidene-1, 1-Bisphosphonate (HEBP) on the formation of dentin and the periodontal attachment apparatus in the mouse. Am J Anat **174**: 83-103.

4. Beertsen W, Neihof A (1986). Root-analogue versus crown-analogue dentin: A radioautographic and ultrastructural investigation of the mouse incisor. Anat Rec **215**: 106-118.

5. Bevelander G, Nakahara H (1966). The formation and mineralization of dentin. Anat Rec **156**: 303-324.

6. Bishop MA, Malhotra M, Yoshida S (1991). Interodontoblastic collagen (von Korff fibers) and circumpulpal dentin formation: An ultrathin serial section study in the cat. Am J Anat **191**: 67-73.

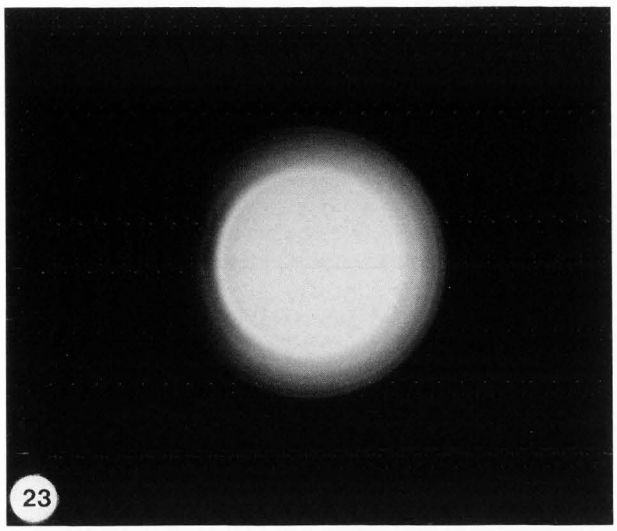

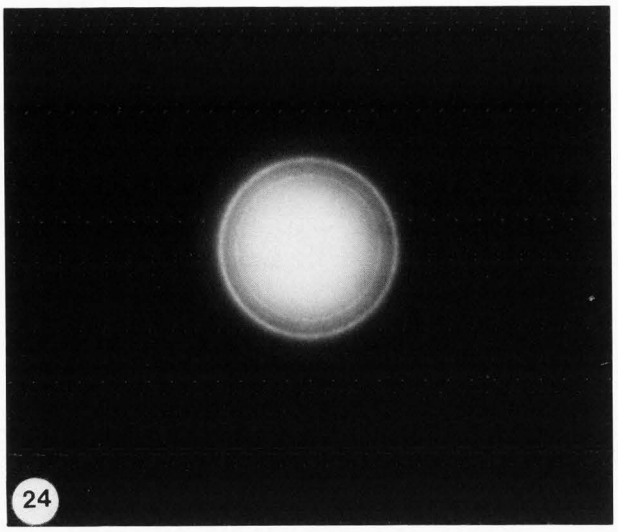

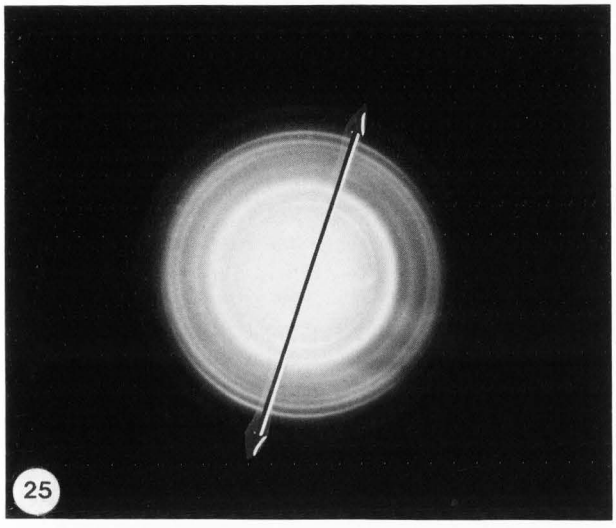

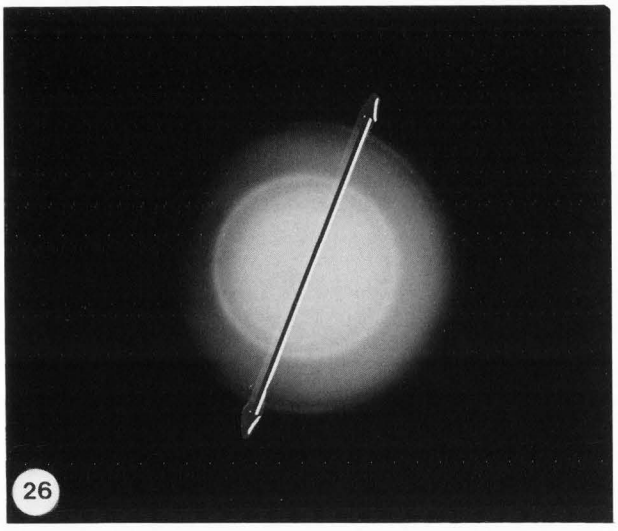

Figures 23-26. Electron diffraction patterns. Labial calcospherites (**Fig. 23**) and lingual calcospherites (**Fig. 24**); root apex. Labial calcospherites (**Fig. 25**) and lingual calcospherites (**Fig. 26**); intermediate region; arrow indicates the direction of the c-axis.

7. Boyde A, Reith EJ (1969). The pattern of mineralization of rat molar dentine. Z Zellforsch **94**: 479-486.

8. Grevstand HJ, Selving KA (1985). Location and ultrastructure of the first cementum formed in rabbit incisors. Scand J Dent Rec **93**: 289-303.

9. Hals E, Tveit AB, Tøtdal B (1988). X-ray microanalysis of dentin: A review. Scanning Microsc **2**: 357-369.

10. Hayashi Y (1984). Crystal growth in calcifying front during dentinogenesis. Acta Anat **118**: 13-17.

11. Hayashi Y, Nagasawa H (1990). Matrix vesicles isolated from apical pulp of rat incisor: crystal formation in low Ca x Pi ion-product medium containing β-Glycerophosphate. Calcif Tiss Int **47**: 365-372.

12. Höhling HJ, Barckhaus RH, Wiesmann HP, Plate U, Reimer L, Boyde A (1992). Different EM - Analytical methods for hard tissue formation. Connec Tiss Res **27**: 81.

13. Jones SJ, Boyde A (1984). Ultrastructure of dentin and dentinogenesis. In: Dentin and Dentinogenesis, Vol. 1, Linde A (ed.), CRC Press, Boca Raton, FL, pp. 81-134.

14. Kakei M, Nakahara H, Kitamura T (1977). An electron microscopic study of the early amelodentinal and cementodentinal junction in the rat incisor. Bull Josai Dent Univ **6**: 7-10.

15. Kogaya Y, Takenaka T, Hatano A, Kato T, Ida A, Tamada H (1978). Electron microscopic studies on the initial formation of Korff's fibrils. J Gifu Dent

Univ **6**: 129-149.

16. Kozawa Y, Terajima T, Mishima H, Sakae T (1989). The intranuclear rodlet in the odontoblast. Nihon Univ J oral Sci **15**: 295-299.

17. Landis WJ, Burke GY, Neuringer JR, Paine MC, Nanci A, Bai P, Warshawsky H (1988). Earliest enamel deposits of the rat incisor examined by electron microscopy, electron diffraction, and electron probe microanalysis. Anat Rec **220**: 233-238.

18. LeGeros RZ (1984). Incorporation of magnesium in synthetic and in biological apatites, In: Tooth Enamel IV, Fearnhead RW, Suga S (eds.), Elsevier, Amsterdam, pp.32-36.

19. LeGeros RZ, Orly I, LeGeros JP, Gomez C, Kazimiroff J, Tarpley T, Kerebel B (1988). Scanning electron microscopy and electron probe microanalyses of the crystalline components of human and animal dental calculi. Scanning Microsc **2**: 345-356.

20. LeGeros RZ, Daculsi G, Kijkowska R, Kerebel B (1989). The effect of magnesium on the formation of apatites and whitockites. In: Magnesium in Health and Disease, Itokawa Y, Durlach J (eds.), John Libbery & Co. Ltd., London, U.K., pp. 11-19.

21. LeGeros RZ (1991). Magnesium in normal and pathological calcifications. In: Mechanisms and Phylogeny of Mineralization in Biological Systems, Suga S, Nakahara H (eds.), Springer-Verlag, Tokyo, pp. 315-319.

22. Lester KS, Boyde A (1968). The question of von Korff fibres in mammalian dentine. Calcif Tiss Res **1**: 273-287.

23. Maejima T (1961). A comparative anatomical study of the dentinal canaliculi in mammals. Acta Anat Nippon **36**: 496-510.

24. Mishima H, Sakae T (1986). Demonstration of structural variation in rat incisor dentin as determined by the X-ray Laue method. J Dent Res **65**: 932-934.

25. Mishima H, Sakae T, Kozawa Y, Hirai G (1988). Structural variation in labial dentin and lingual dentin in the rat incisor. J Nihon Univ Sch Dent **30**: 1-10.

26. Mishima H, Kozawa Y, Sakae T (1991). Two patterns of calcification in rat and rabbit incisor dentin. In: Mechanisms and Phylogeny of Mineralization in Biological Systems, Suga S, Nakahara H (eds.), Springer-Verlag, Tokyo, pp. 223-227.

27. Mishima H, Sakae T, Kozawa Y (1991). Morphological study of calcospherites in rat and rabbit incisor dentin. Scanning Microsc **5**: 723-729.

28. Mummery JH (1924). Calcification. In: The Microscopic and General Anatomy of the Teeth, 2nd edn., Humphrey Milford Oxford University Press, London, pp. 124-142.

29. Numata T, Mishima H (1991). Histology of the incisor dentin of the rabbit supplemented with X-ray Laue method. Nihon Univ J oral Sci **17**: 20-31.

30. Okazaki M, Takahashi J, Kimura H (1986). Unstable behavior of magnesium-containing hydroxyapatites. Caries Res **20**: 324-331.

31. Okazaki M (1987). Mg^{2+}-F^- interaction during hydroxyapatite formation. Magnesium **6**: 296-301.

32. Okazaki M (1991). Crystallographic behavior of iron and magnesium in hydroxyapatite crystals. In: Mechanisms and Phylogeny of Mineralization in Biological Systems, Suga S, Nakahara H (eds.), Springer-Verlag, Tokyo, pp. 309-313.

33. Onozato H, Watabe N (1979). Studies on fish scale formation and resorption. III. Fine structure and calcification of the fibrillary plates of the scales in *Carassius auratus* (Cyprinformes: Cyprinidae). Cell Tissue Res **201**: 409-422.

34. Rosenberg GD, Simmons DJ (1980). Rhythmic dentinogenesis in the rabbit incisor: Allometric aspects. Calcif Tiss Int **32**: 45-53.

35. Schmidt WJ, Keil A (1958). Die gesunden und die erkrankten Zahngewebe des Menscen und der Wirbeltiere im Polarisatiosmikroskop (Polarizing Microscopy of Dental Tissues). Carl Hanser Verlag, München, pp. 45-127.

36. Schonfeld SF, Slavkin HC (1977). Demonstration of enamel matrix proteins on root-analogue surfaces of rabbit permanent incisor teeth. Calcif Tiss Res **24**: 223-229.

37. Shellis RP (1983). Structural organization of calcospherites in normal and rachitic human dentine. Archs oral Biol **28**: 85-95.

38. Shimahara T (1986). Histological and histogenetic studies on the outermost layer of dentine in the molar teeth of the rat. Tsurumi Shigaku **12**: 160-188.

39. Steinfort J, van den Bos T, Beertsen W (1989). Differences between enamel-related and cementum-related dentin in the rat incisor with special emphasis on the phosphoproteins. J Biol Chem **264**: 2840-2845

40. Steinfort J (1990). The Possible Role of Non-Collagenous Matrix Components in Dentin Mineralization. The Rat Incisor as a Model. Kaal Boek, Amsterdam, pp. 102-106.

41. Tanaka S (1987). On the regional dimorphism of young odontoblasts in rat teeth. Acta Anat Nippon **62**: 626-639.

42. Ten Cate AR (1989). Dentinogenesis. In: Oral Histology, Development, Structure, and Function. 3rd edn., The CV Mosby Company, St. Louis, pp. 139-156.

Discussion with Reviewers

M.B. Engel: What is the role of dentin ground substance in calcification [cf. Engel MB, Hilding OH (1984). Mineralization of Developing Teeth, Scanning Electron Microsc **1984**; IV: 1833-1845]?

Authors: We assume that dentin ground substance is related to the initial nucleation of dentin crystal. We think that phosphophoryn may be responsible for the nucleation event in the mineralizing calcospherite.

M.B. Engel: Do the authors have results for the uncalcified matrix continuous to the calcospherites?

Authors: Yes, we have. By TEM-EDS analysis, Na, Si, P, S, K and Ca were detected in small amounts.

M.B. Engel: Do the fixation procedures affect the localization and, or, the element concentration?
Authors: Yes, there is a slight possibility that they affect the localization and the element concentration.

J. Appleton: What are the factors which determine the range of sizes of calcospherites during the development of dentine?
Authors: It is considered that the activity of odontoblast and the local environment of predentin may determine the range of sizes of calcospherites.

J. Appleton: What are the dynamic mechanisms which alter the calcospherite configuration as the tooth is worn at the incisal edge and new tissue generated at the apex?
Authors: It is assumed that the alteration of calcospherite configuration may possibly arise from a different pattern of calcification.

R.P. Shellis: Although your Ca/P ratios agree with reported values for carbonate-apatites, they are much higher than those found by analysis of dentine, which are lower than 1.67 [Rowes SL (1967) In: Structural and Chemical Organization of Teeth. Vol. 2, Miles AEW (ed.), Academic Press]. Can you explain this discrepancy?
Authors: Calcospherites in predentin are not completely calcified. We assume that the difference in Ca/P ratios is related to the difference in the degree of calcification.

R.P. Shellis: How sensitive is your electron-diffraction technique to non-apatitic phases such as OCP?
Authors: Our electron-diffraction analysis is quite sensitive. Our results agree with the findings of Höhling *et al.* [12].

R.P. Shellis: Did you observe matrix vesicles in the predentin and if so, would their distribution be consistent with the hypothesis [37] that calcospherite formation may be initiated by matrix vesicles?
Authors: No, these matrix vesicles were not observed in secondary circumpulpal dentinogenesis. We think that matrix vesicles do not participate in calcospherite formation of circumpulpal dentin.